Plasma anisotropy around a dust particle placed in an external electric field

G. I. Sukhinin,[1,2,3,*] A. V. Fedoseev,[1,3] M. V. Salnikov,[1] A. Rostom,[2] M. M. Vasiliev,[3] and O. F. Petrov[3]
[1]*Institute of Thermophysics, 630090 Novosibirsk, Russia*
[2]*Novosibirsk State University, 630090 Novosibirsk, Russia*
[3]*Joint Institute for High Temperatures, 125412 Moscow, Russia*
(Received 17 April 2017; published 29 June 2017)

A self-consistent model of plasma polarization around an isolated micron-sized dust particle under the action of an external electric field is presented. It is shown that the quasineutral condition is fulfilled and the formed volume charge totally screens the dust particle. The ion focusing and wake formation behind the dust particle are demonstrated for different ion mean free paths and the external electric fields. It is obtained that at low values of the external electric field the trapped ions play the main role in the screening of the dust particle charge. For high external electric fields, the density of trapped ions decreases and the dust particle is screened mainly by the free ions.

DOI: 10.1103/PhysRevE.95.063207

I. INTRODUCTION

Dusty plasma is an ionized gas that contains solid dust particles [1–4]. In gas discharge plasma, the dust particles are normally highly charged by electron and ion fluxes on their surface. The negatively charged dust particles usually form a cloud of particles confined by the external electric field. They strongly interact with each other and can form an ordered structure of particles, such as chains or crystals (hexagonal monolayers) [5–7]. Usually, to describe the phenomenon of dust particle interaction it is assumed that a single isolated particle interacts with other particles via screened Coulomb potential, i.e., Debye-Hückel potential. It is shown that the Debye-Hückel potential is a good approximation for a screened charge potential and makes it possible to describe many experimental results [8–11]. Such isotropic potential distribution is useful for qualitative analytical and numerical investigations of the collective structural and dynamical processes in a complex plasma and self-organization of dust particles in screened systems with strong interaction between the particles [12–17].

In most cases typical of gas discharge plasma, dust particles are located in a plasma flow driven by an external electric field (strong electric fields in the electrode layer of rf discharge or in striations of dc discharge). In the presence of the plasma flow around a dust particle, nontrivial effects arise. One of the most common and significant phenomena is the ion flux focusing behind the dust particle [18–28]. In this case, the spatial distribution of the electric potential around the dust particle becomes anisotropic. Behind the dust particle a so-called wake effect [18–36] appears, i.e., an oscillated electric potential arises downstream of the ion flow.

The plasma flow produced by the action of the external electric field breaks the spherical symmetry of the plasma parameters around the dust particle and makes the problem difficult for analytical consideration. The most common methods for investigating this effect are a linear response (LR) method [21,32,37–39] and a "particle-in-cell" (PIC) method [19,22,24–28,33–35,40–42], which permit one to take into account the multicomponent and multiparametric nature of the problem.

In a lot of presented numerical models, a dust particle is presented as a pointlike or a finite-sized particle with a fixed charge. In such models, the electron and ion absorbtion by the dust particle are usually neglected, and the charge of the particle does not correspond to its floating potential. This means that the processes of dust particles charging in a plasma flow is not taken into account and the condition of quasineutrality in the plasma around dust particles is not satisfied. As a consequence, spatial distributions of ion density and plasma potential cannot be properly considered.

In the paper, a micron-sized dust particle is considered for typical laboratory dusty plasma conditions. In order to describe the effect of plasma polarization around the dust particle under the action of an external electric field, a self-consistent model is developed. In the model, the process of dust particle charging and the formation of ion density and electric potential spatial distributions around the dust particle are considered. The description of the model is presented in Sec. II. The results of the calculations are presented in Sec. III. Finally, a conclusion is presented in Sec. IV.

II. MODEL

A system of an isolated highly charged dust particle and surrounding plasma of electrons and ions under the action of an external electric field is considered. The clouds of electrons and ions of this system screen the dust particle charge. Ion trajectories are calculated by the Newtonian motion equations in the Cartesian coordinate system. They are simulated inside a three-dimensional (3D) cubical region with dimensions equal to $2L$ in each direction, where $L = 20\lambda_i$, $\lambda_i = [(kT_i)/(4\pi e^2 n_i)]^{1/2}$ is the ion Debye length, and n_i and T_i are the ion density and temperature of the unperturbed plasma, correspondingly. In the center of the system the absorbing sphere of radius $r_0 \ll \lambda_i$ is placed, which models the negatively charged dust particle. The electric field (E_z) is directed along the z axis.

At the very beginning of the calculations, an ion is generated with random position inside the solution region. A random initial velocity is assigned to this ion corresponding to a

*sukhinin@itp.nsc.ru

Maxwell velocity distribution with the ion mean temperature, $T_i = 300$ K. Monte Carlo simulations are used to determine the initial coordinates of each ion, its initial velocity distribution, and its free path, $\boldsymbol{l}$. At every time step, a new position of the ion is determined with the help of Newtonian motion equations, and the following conditions are checked: if the ion leaves the solution region ($|x|,|y|,|z| > L$), if the ion falls on the particle surface ($r \leqslant r_0$), and if the ion passes its free path. The realization of the last condition means that a resonant charge exchange process between the ion and a neutral atom (argon) takes place. For each particular ion its free path $\boldsymbol{l}$ is generated according to the exponential distribution, which depends on the ion mean free path $\bar{l}_i$. The ion mean free path $\bar{l}_i$ is determined by the effective cross section of the resonant charge exchange processes, $\sigma_{\rm res}$. Our model implies $\sigma_{\rm res}$ to be constant: $\sigma_{\rm res} = 55.3 \times 10^{-16}{\rm cm}^2$ (it practically does not depend on the velocity of ion-neutral atom collisions [43,44]). The processes of nonresonant elastic collision of the ion with a neutral atom and ion-ion collisions are neglected due to small values of their frequencies. After each charge exchange collision, a new random velocity of the ion is generated according to the Maxwell velocity distribution, while the position of the ion remains the same. When the ion reaches the solution region edge, it is injected in the opposite side of the region at the same velocity as before leaving the solution region. When the ion falls on the dust particle, a new ion is generated with random coordinates and random velocities.

The 3D trajectory of the ion movement, i.e., the components of the ion's position and its velocity, and the components of forces acting on the ion are calculated in Cartesian coordinates. However, spherical coordinates (r, θ, φ) are introduced to calculate the ion density spatial distribution $n_i(r,\theta,\varphi)$. The angle $\theta = 0$ corresponds to the direction of the external electric field $\overrightarrow{E} = (0,0,E_z)$, and $z = r\cos\theta$. Due to cylindrical symmetry of the problem, there are no dependencies of plasma parameters on the angular coordinate φ. The solution region is divided into spatial cells indexed by (i,j), with volume equal to $V_{i,j} = 2\pi r_i^2 \Delta r_i \sin\theta_j \Delta\theta_j$ ($i = 1,2,\ldots,60$; $j = 1,2,\ldots,31$). The time $T_{i,j}$ that ions spend in each particular cell (i,j) is *accumulated*, and normalized to the cell volume. It is assumed that the density of ions, $n_i(r_i,\theta_j)$, is proportional to this normalized time. The coefficient of proportionality is determined by the nonperturbed ion density n_∞ far from the dust particle, i.e., at the boundary of the solution region, $r = L$. The mean velocity of the ions in each spatial cell can be found in the same way.

The spatial distribution of electron density is assumed to obey the Boltzmann distribution, $n_e(r,\theta) \sim n_\infty \exp(U(r,\theta)/kT_e)$, where $U(r,\theta)$ is the spatial distribution of the electric potential and T_e is the electron temperature. Ions move near the dust particle under the action of forces induced by potentials of the dust particle charge $-eZ_d$, the volume charge of ions and electrons, $e(n_i(r,\theta) - n_e(r,\theta))$, and the external electric field E_z.

For calculations, the following dimensionless parameters are used. All spatial dimensions are normalized to the ion Debye length λ_i. The densities of electrons and ions are measured in units of nondisturbed plasma density far from the dust particle, n_∞. Energy quantities are normalized to the ion thermal energy kT_i. Velocities and times are normalized to the ion thermal velocity $V_T = \sqrt{kT_i/M}$ and $T = \lambda_i\sqrt{M/kT_i}$, where M is the ion mass. Thus, the dimensionless particle charge $\widetilde{Q}$ and the external electric field strength $\widetilde{E}$ are the following:

$$\widetilde{Q} = \frac{Z_d e^2}{\lambda_i kT_i}, \quad \widetilde{E} = \frac{e\lambda_i E_z}{kT_i}. \tag{1}$$

Along with $\widetilde{Q}$, the following dimensionless representation of particle charge is often used:

$$\widetilde{z} = \widetilde{Q}\frac{T_i\lambda_i}{T_e r_0} = \frac{Z_d e^2}{kT_e r_0}. \tag{2}$$

The effective electric field or a dimensionless form of a reduced electric field is also introduced:

$$E_{\rm eff} = (e\bar{l}_i E_z)/(kT_i) \sim E_z/n_{\rm gas} \sim E_z/p, \tag{3}$$

where p is the gas pressure.

To start the calculation, the initial distribution of an electric potential is used as a sum of the potential induced by the external electric field and the Debye-Hückel potential:

$$U^0(r,\theta) = -(\widetilde{Q}/r)\exp(-r). \tag{4}$$

In a weak external electric field, the spatial distributions of electron density $n_e(r,\theta)$ and ion density $n_i(r,\theta)$ and the self-consistent electric potential $U(r,\theta)$ have a weak anisotropy due to the action of the external electric field E_z. These distributions can be found with the help of expansions of these distributions in Legendre polynomials (harmonics). The dimensionless density of volume charge spatial distribution, $n(r,\theta) = [n_i(r,\theta) - n_e(r,\theta)]/n_\infty$, can be presented in the following form:

$$n(r,\theta) = \sum_{k=0} n_k(r) P_k(\cos\theta), \tag{5}$$

$$n_k(r) = \frac{(2k+1)}{2}\int_0^\pi n(r,\theta) P_k(\cos\theta)\sin\theta\, d\theta. \tag{6}$$

For the case of a weak external electric field, i.e., for $\widetilde{E} < 0.1$, only the first three terms are enough to describe the spatial distribution $n(r,\theta)$. For high values of the electric field $\widetilde{E} > 1$ it is necessary to take into account up to eight or even more expansion terms. The terms $n_{0,1,2}(r)$ are the isotropic, dipole, and quadruple harmonics of volume charge density. After calculating n_k, the electric potential spatial distribution can be found in the form of the following expansion:

$$\begin{aligned} U(r,\theta) &= -\frac{\widetilde{Q}}{r} + \sum_{k=0} U_k(r) P_k(\cos\theta) \\ &= -\frac{\widetilde{Q}}{r} + \sum_k \frac{1}{2k+1} P_k(\cos\theta) \\ &\quad \times \left[\frac{1}{r^{k+1}}\int_{r_0}^r x^{k+2}\, dx n_k(x) + r^k \int_r^\infty dx \frac{n_k(x)}{x^{k-1}}\right]. \end{aligned} \tag{7}$$

The ion trajectories under the action of the self-consistent electric potential are calculated with the help of dimensionless

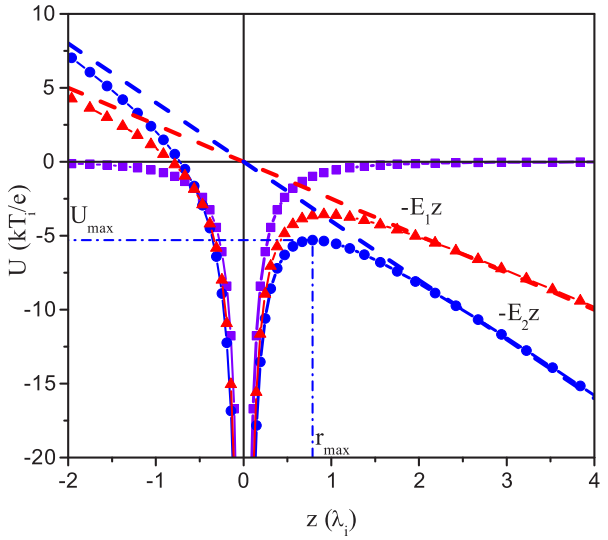

FIG. 1. Electric potential $U(\rho = 0,z) - \widetilde{E}z$ in the presence of an external electric field.

Newtonian equations:

$$\frac{d^2 r_\alpha}{dt^2} = -\frac{\partial(U(r,\theta) - \widetilde{E} r\cos\theta)}{\partial r_\alpha}, \tag{8}$$

where $\alpha = x,y,z$. These equations are solved by the fourth-order Runge-Kutta method.

The model permits one to divide ion density into two groups: the densities of trapped and free ions. The total energy of each particular ion can be found by the formula

$$E_{\text{tot}} = \varepsilon_k + U(r,\theta) - Ez, \tag{9}$$

where ε_k is the ion kinetic energy.

In the absence of an external electric field, the trapped ions have negative total energy, $E_{\text{tot}} < 0$, and free ions have positive total energy, $E_{\text{tot}} > 0$. If the potential of the external electric field $-\widetilde{E}z$ is added to the potential of the dust particle and surrounding plasma, $U(r,\theta)$, a local maximum of the potential, $U_{\max}(r_{\max},\theta_{\max})$, located at a distance $r_{\max}$ from the dust particle, appears downstream of the dust particle (see Fig. 1). The ions for which the total energy E_{tot} is lower than $U_{\max}$ and the position r is less than $r_{\max}$ are trapped ions and the rest are free.

The isotropic term $n_0(r)$ determines the total volume charge of plasma around the dust particle Q_{pl}:

$$Q_{\text{pl}} = \frac{1}{2}\int_0^\infty \int_0^\pi n(r,\theta) r^2 \sin\theta\, d\theta\, dr = \int_0^\infty n_0(r) r^2\, dr. \tag{10}$$

The total volume charge Q_{pl} obtained by Eq. (10) becomes equal to the charge $\widetilde{Q}$ of the dust particle, which is calculated self-consistently equating the electron and ion fluxes on the dust particle surface. This equality proves that the model is self-consistent.

Under the action of the external electric field, the positively charged ion cloud shifts relative to the negatively charged dust particle, and the appearance of a dipole moment of this system is expected:

$$\widetilde{P} = \frac{eP}{kT_i\lambda_i^2} = \frac{1}{2}\int_0^\infty \int_0^\pi n(r,\theta) r^3 \cos\theta \sin\theta\, d\theta\, dr = \frac{1}{3}\int_0^\infty n_1(r) r^3\, dr, \tag{11}$$

where $\widetilde{P}$ is a dimensionless dipole moment.

To obtain the self-consistent electric potential distribution of the dust particle–ion cloud system, the following calculation algorithm is adopted. First of all, the ion trajectories under the action of forces are calculated with the help of Newtonian equations (8) for the electric potential taken in form (4). When sufficient statistical data for ion spatial distribution $n_i(r,\theta)$ are obtained, the expansion terms n_k are calculated with the help of Eq. (6). Then, a new spatial distribution $U(r,\theta)$ is calculated [Eq. (7)]. The calculation procedure is repeated and new statistical data for ion density spatial distribution in this new potential distribution are found. At each iterative step, the charge of the dust particle, $\widetilde{Q}$, is found equating the electron and the ion fluxes on the particle surface, which is equal to the volume charge of plasma, Q_{pl} [Eq. (10)]. The iterative process continues until the spatial distributions of the electric potential $U(r,\theta)$ and the ion density $n_i(r,\theta)$ as well as the dust particle charge $\widetilde{Q}$ stop changing. The time between the iterations is determined by the accumulated statistics. It should be stressed that the final distributions do not depend on the choice of the initial potential distribution.

In this paper precise calculations in the vicinity of a relatively small dust particle were performed in the region of several decades of ion Debye lengths λ_i. Ions and electrons move around the dust particle in opposite directions with corresponding drift velocities in the external electric field. The speed of neutral atoms is isotropic, in contrast to numerous studies [25,35,42] where the charged dust particle moves in plasma relative to static ions, electrons, and neutral atoms. In the case when the dust particle moves in plasma, when the processes of a resonant charge exchange collision of an ion and a neutral atom is simulated, a new ion has a velocity corresponding to a shifted Maxwell distribution; i.e., it has the velocity of the neutral atom before its collision with the ion. In this model, the drift velocity of neutrals relative to the dust particle is equal to zero, and the recharged ion has the isotropic velocity distribution.

It should be noted that the model does not take into consideration the interaction between all ions and electrons in the system, but it studies the approximation of an average field. The self-consistent spatial distribution of the electric potential [Eq. (7)] is calculated by taking into account the spatial distribution of the volume charge [Eq. (5)] not at every ion time step. It is recalculated after statistical data on ion density are accumulated in the course of 1×10^6–1×10^8 ion free paths. It makes it possible to considerably speed up the calculation of the potential. Moreover, the simulation can be carried out at different computer stations simultaneously, synchronizing calculations from time to time by introducing a new iteration for the distribution of the electric potential.

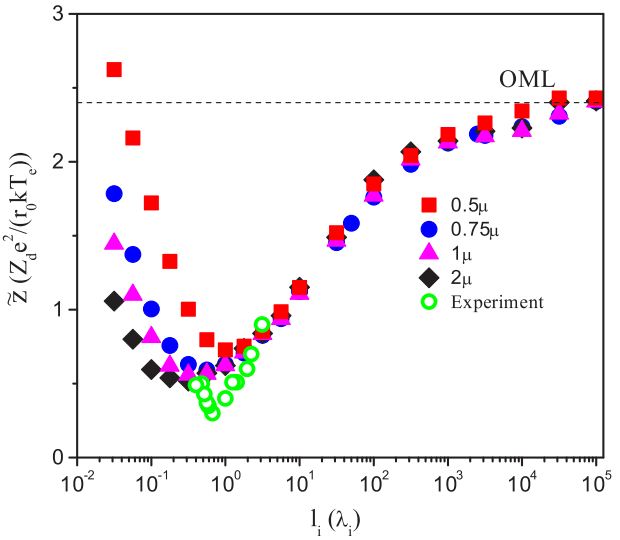

FIG. 2. Dimensionless dust particle charge in the absence of an external electric field for different ion mean free paths $\bar{l}_i$ and dust particle radii r_0. Experimental results are presented in Ref. [25] for the particle with radius 0.6 μm.

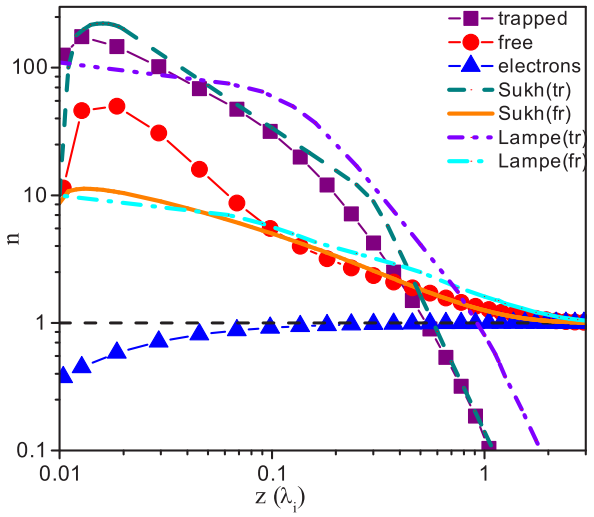

FIG. 3. Bulk charge density $n(\rho = 0,z)$ for electrons and different kinds of ions for $E_{\text{eff}} = 0$ and $\bar{l}_i/\lambda_i = 5$. Solid lines show the results obtained in previous work [47].

III. RESULTS

In the paper, typical conditions for argon gas discharge plasma with an isolated dust particle are considered. It is assumed that the electron temperature is equal to $kT_e = 3$ eV, and ions are at room temperature $kT_i \approx 0.03$ eV, parameter $\tau = T_e/T_i = 100$, $T_g = T_i$. The ion Debye screening length is equal to $\lambda_i = 1 \times 10^{-2}$ cm which corresponds to plasma density of about $n_\infty \approx 1 \times 10^8$ cm^{-3}. The dust particle radius is equal to $r_0 = 1 \times 10^{-4}$ cm $= 1 \times 10^{-2}\lambda_i$.

The dimensionless dust particle charge $\widetilde{z}$ was calculated self-consistently depending on the ion mean free path $\bar{l}_i$ in argon in the absence of an external electric field (see Fig. 2). In the limit $\bar{l}_i \to \infty$, the dimensionless charge of the dust particle $\widetilde{z}$ tends to be a constant with value 2.4 that coincides with the value obtained with the help of the orbital motion limited (OML) model [45]. The presence of the minimum in the dependence $\widetilde{z}(\bar{l}_i/\lambda_i)$ can be described in terms of ion flux to the dust particle from the plasma. In the OML model (a free molecular regime), collisionless ions rarely fall on the micron-sized dust particle. With the increase of gas density (decrease of ion mean free path), ions collide more frequently with neutral atoms around the dust particle. After a resonant charge exchange collision, a positively charged ion loses its kinetic energy and it is easily attracted by the negatively charged dust particle. Thus, the total ion flux towards the dust particle increases with the increase of ion collision frequency. However, with a further decrease of the ion mean free path, the falling ions take part in many collisions before they fall on the dust particle. The ions lose their kinetic energy several times, which leads to the increase of the average falling time and to the decrease of the total ion flux to the particle. Thus, the minimum in charge dependence $\widetilde{z}(\bar{l}_i/\lambda_i)$ appears.

It should be mentioned that in many papers [25–28,46] dust particle charge was calculated by another collisional model for the case of the absence of the external electric field. It was assumed that the ion-neutral atom collision frequency is independent of their relative velocity. In our opinion, the model with a constant collision cross section is more suitable for describing the resonant charge exchange collisions of ions in parent noble gases. However, both models are approximations and show qualitatively the same charge dependencies on gas pressure.

The two-dimensional spatial distributions of the dimensionless volume charge density $n(\rho,z) = [n_i(\rho,z) - n_e(\rho,z)]/n_\infty$ are obtained for different values of the external electric field and ion mean free path. In Fig. 3, the radial distributions of the density of free and trapped ions and electrons are presented for the external electric field $E_{\text{eff}} = 0$ and mean free path $\bar{l}_i = 5\lambda_i$. The form and the value of the peak are in good agreement with the data obtained earlier by applying non-self-consistent models in Refs. [47–49].

In the presence of the external electric field $E_{\text{eff}} > 0$, the spherical symmetry of plasma parameters around the dust particle is broken; however, cylindrical symmetry is fulfilled. All distributions of the plasma parameters stretch along the external electric field and can be presented in cylindrical coordinates ρ and z. At the beginning of the calculations, we accumulate some statistical data on the volume charge spatial distribution for spherically symmetric electric potential [Eq. (4)] in the presence of the electric field. The obtained distribution of the volume charge density $n(r,\theta)$ around the dust particle can be analyzed with the help of expansion into Legendre polynomials [Eqs. (5) and (6)]. The terms of expansion, $n_k(r)$, or harmonics, were calculated for different values of the external electric field strength E_{eff} and for different ion mean free paths $\bar{l}_i$. All terms $n_k(r)$ depend only on the distance from the dust particle, r, and the dependence of plasma density on the angle θ is determined by Eq. (5). In Figs. 4(a) and 4(b), the first two terms $n_0(r)$ and $n_1(r)$ multiplied by the factors r^2 and r^3, correspondingly, are presented. These two harmonics play a specific role for plasma distribution around a dust particle in an external electric field. The integral of the zeroth harmonic, $\int_{r_0}^{\infty} n_0(r) r^2 dr$, determines

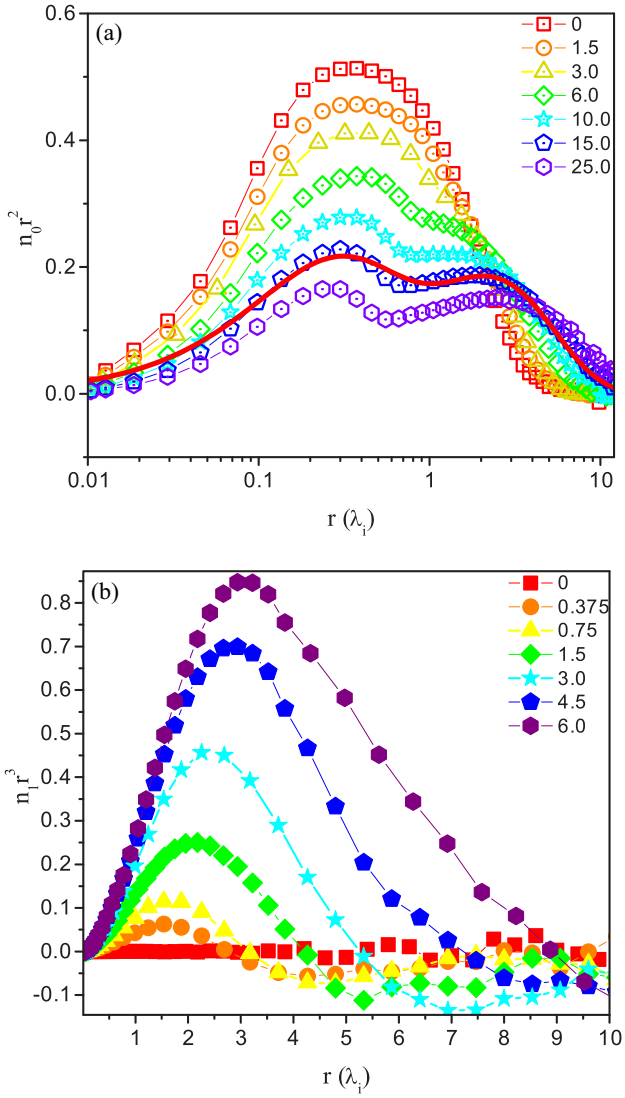

FIG. 4. Functions (a) $n_0(r)r^2$ and (b) $n_1(r)r^3$ for $\bar{l}_i/\lambda_i = 5$ and different values of E_{eff}. The solid line indicates the Debye approximation function.

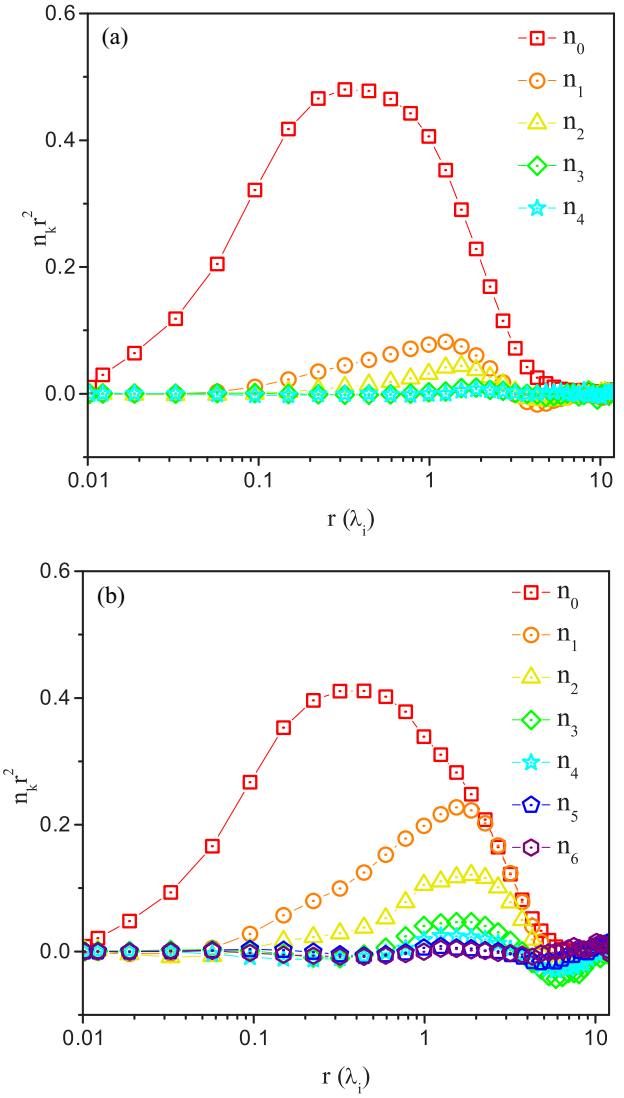

FIG. 5. Functions $n_k(r)r^2$ for $\bar{l}_i/\lambda_i = 5$: (a) $E_{\text{eff}} = 0.75$ and (b) $E_{\text{eff}} = 3.0$.

the volume charge Q_{pl} of plasma around the dust particle according to Eq. (10). The integral of the first harmonic, $\int_{r_1}^{\infty} n_1(r)r^3 dr$, determines the dipole moment of the dust particle–ion cloud system according to Eq. (11).

It is seen that for small values of the electric field, the function $n_0(r)r^2$ has one hump in the vicinity of the dust particle, $r_{1\,\max} \simeq (0.3 - 0.5)\lambda_i$. This maximum means that the distribution of trapped ions around the dust particle has a shell structure like in a "quasiatom" with a negative core [47]. The dependencies calculated in Ref. [47], $N_{\text{tr}}(r)r^2$, have approximately the same radial distributions as $n_0(r)r^2$, where $N_{\text{tr}}(r)$ is the radial distribution of the trapped ion density. It is concluded that the majority of the trapped ions are concentrated in the layer or shell around $r_m \sim (0.3\text{–}0.5)\lambda_i$. It can be shown that the ions taking part in resonant charge exchange collisions at distances smaller than approximately $2.5\lambda_i$ acquire negative total energy and can be attributed to trapped ions. However, at very high values of the electric field, the second hump in the radial distribution of $n_0(r)r^2$ appears at larger distances, $r_{2\,\max} \simeq (2.0\text{–}4.0)\lambda_i$. Such a "camel-like" structure of distribution $n_0(r)r^2$ can be approximated by the superposition of two Debye functions with different screening length: $\lambda_1 \leqslant \lambda_i$ and $\lambda_2 > \lambda_i$ [see Fig. 4(a)].

In Fig. 4(b), radial distributions $n_1(r)r^3$ are presented. For zero electric field strength all anisotropic terms $n_{k>0}(r)$ of the expansion into the Legendre polynomials are equal to zero. At small values of the electric field, the anisotropic harmonic $n_1(r)$ appears and increases linearly with the increase of electric field strength. It is seen that with a further increase of the electric field ($\widetilde{E} > 0.5$), an oscillatory structure in $n_1(r)$ appears in the region $r > \lambda_i$, which is a precursor for a wake formation behind the dust particle. However, in this remote region, the values of $n_1(r)$ become very small [$n_1(r) < 10^{-4} n_\infty$]. For the region $r > 10\lambda_i$ the function $n_1(r)r^3$ is fully masked by noise, and there is no opportunity to calculate any integral with reliable precision. The radial position of maxima in $n_1(r)$ dependencies shifts to higher distances from the dust particle with the increase of the electric field. For small values of the electric field, the maximum

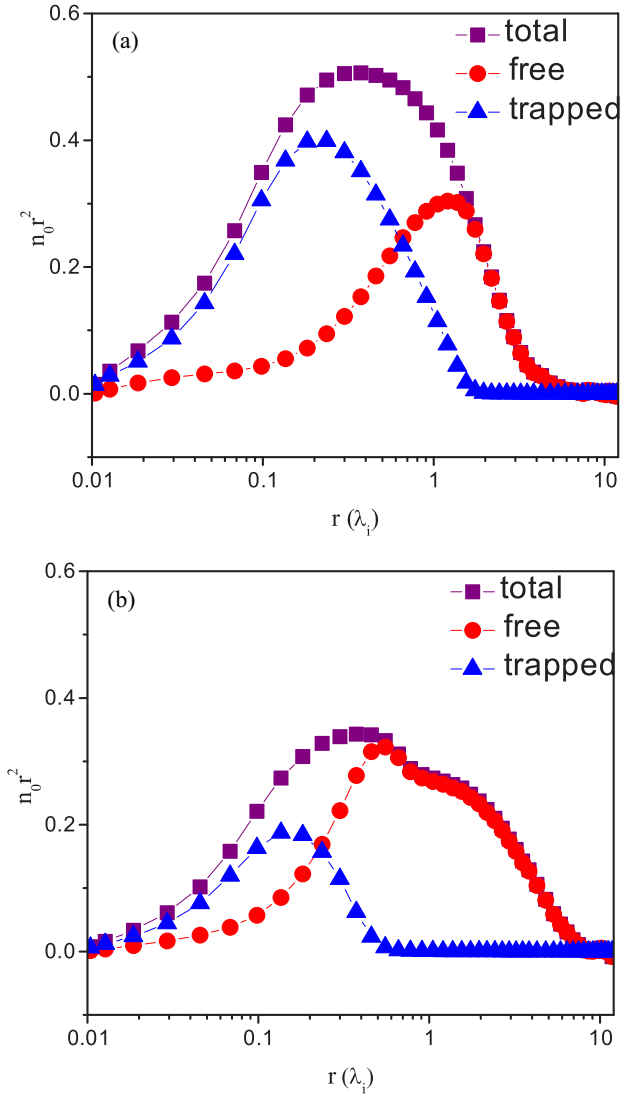

FIG. 6. Function $n_0(r)r^2$ for $\bar{l}_i/\lambda_i = 5$: (a) $E_{\text{eff}} = 0.0$ and (b) $E_{\text{eff}} = 6.0$ for different sorts of ions.

values of $n_1(r)r^3$ have a linear dependence on the electric field strength.

In Figs. 5(a) and 5(b), radial distributions $n_k(r)r^2$ are presented for the external electric fields $E_{\text{eff}} = 0.75$ and $E_{\text{eff}} = 3.0$, correspondingly. It is shown that the external field leads to the appearance of harmonics with number $k > 0$. The greater the electric field, the greater the number of harmonics, which take part in the formation of a self-consistent electric potential. In Fig. 5(a) ($E_{\text{eff}} = 0.75$) it is seen that harmonics with number $k > 3$ may be omitted. In Fig. 5(b) ($E_{\text{eff}} = 3.0$) it is shown that all harmonics with $k \geqslant 1$ are higher and harmonics up to fifth must be considered.

A dust particle surrounded by a cloud of trapped ions forms a "quasiatom." Without the external electric field, trapped ions play the main role in the screening. This can be seen in Fig. 6(a). They also provide most of the volume charge. In the presence of the external field, trapped ion density decreases, which can be interpreted as quasiatom ionization [see Fig. 5(b)]. However, with the increase of the electric field,

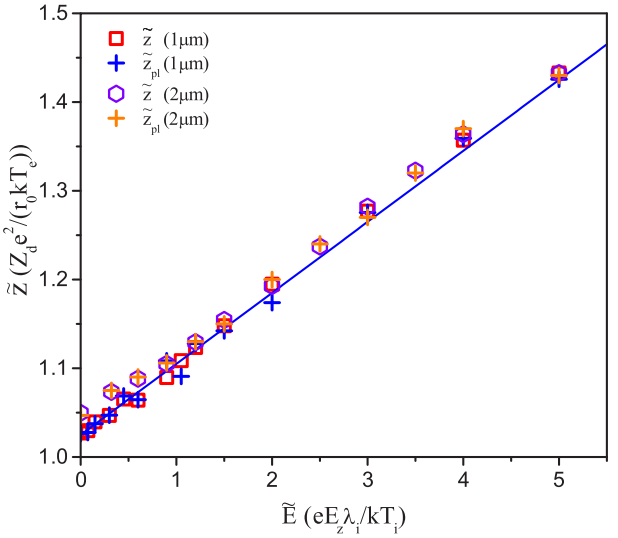

FIG. 7. Dependence of dimensionless charges z_{pl} and $\tilde{z}$ from dimensionless electric field $\tilde{E}$ for $\bar{l}_i/\lambda_i = 5$ and different particle radii.

the dust particle charge and the volume charge of surrounding plasma increase and free ions begin to play the main role in the screening of the dust particle.

It should be noted that the dust particle charge $\tilde{z}(\tilde{E})$ and the volume charge $z_{\text{pl}}(\tilde{E})$ are equal to each other for any values of the electric field strength and ion mean free path (Fig. 7). This means that the formed volume charge totally screens the dust particle charge placed in the plasma. Both functions have linear dependence on the external electric field strength. In the absence of the electric field, $\tilde{E} = 0$, the dust particle charge has the value $\tilde{z}(\tilde{E} = 0) \approx 1.03$ (see Fig. 2).

Finally, we obtain a self-consistent electric potential distribution $U(\rho,z)$, which is presented in Figs. 8(a) and 8(b) for different values of the electric field strength E_{eff} and particle radius ($r_0 = 1$ and 2μm). In the absence of the external electric field, $E_{\text{eff}} = 0$, the electric potential and the bulk charge are spherically symmetric, and the left and right branches of $U(\rho = 0,z)$ [see Figs. 8(a) and 8(b)] and the density of volume charge $n(\rho = 0,z)$ are symmetric. In the presence of the external electric field, $E_{\text{eff}} > 0$, ion trajectories skew along the action of the electric field, i.e., to the right side of axis z. The spatial asymmetry of the bulk charge $n(\rho,z)$ leads to the asymmetry of the electric potential spatial distribution $U(\rho,z)$, which is calculated with the help of Eq. (7). The results show that for high values of the external electric field, the positive peaks of the electric potential appear downstream of the dust particle, $z > 0$ and $\rho = 0$. For the ion mean free path $\bar{l}_i = 5\lambda_i$ and external electric field $E_{\text{eff}} = 6.0$, the maximum in the electric potential spatial distribution is located around the point $z \simeq 4$, $\rho = 0$. This positive peak of the potential is the beginning of the wake and it is formed exclusively by free ions.

The maximum value of this peak $U_{\max}(z,\theta = 0)$ initially increases linearly with the increase of the electric field, and then turns into the regime of saturation (Fig. 9). At the same time, the upstream part of the potential curve becomes wider. For a larger radius of the dust particle (and larger charge), the maximum of the potential peak increases with almost the same

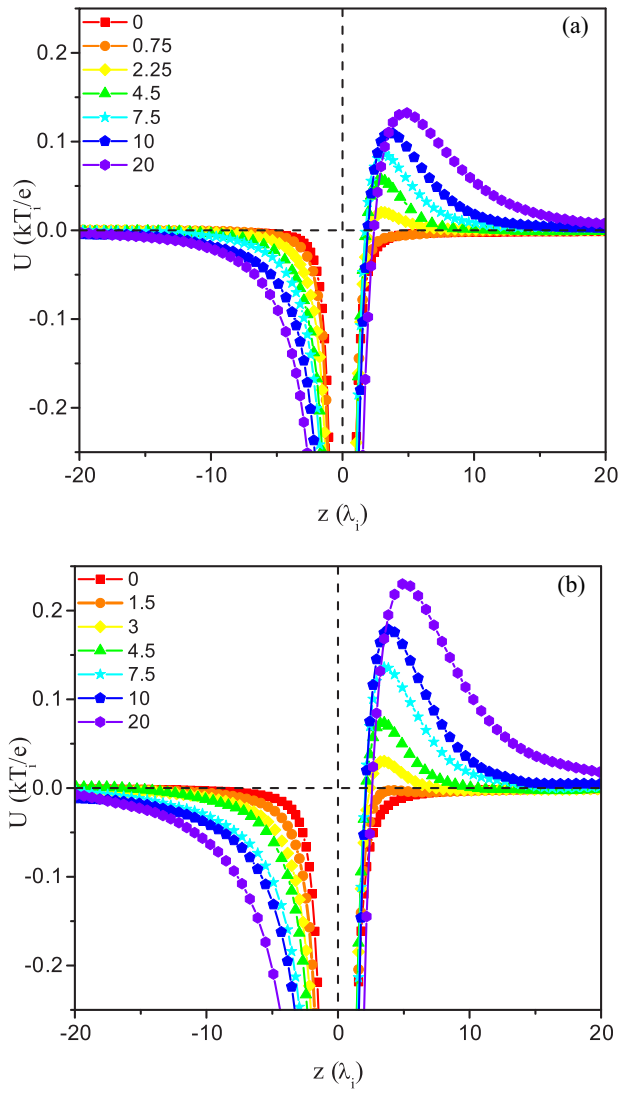

FIG. 8. Electric potentials $U(\rho = 0,z)$ for (a) $r_0 = 1\mu$ and (b) $r_0 = 2\mu$, $\bar{l}_i/\lambda_i = 5$, and different values of E_{eff}.

rate but with larger saturation limit. For small values of the external electric field ($\widetilde{E} < 0.6$), this peak is not proportional to the charge of the dust particle. Only for large values of the external electric field ($\widetilde{E} > 1$) can one say that the magnitudes of the potential peaks are approximately proportional to the radius of the dust particle. The results show that the calculated self-consistent spatial potential distribution (i.e., magnitude, shape, and behavior of the wake) depends on the dust particle radius (or charge).

These positive peaks in the electric potential spatial distributions $U(\rho,z)$ play the role of electric potential wells for negatively charged particles. For example, if we place another negatively charged dust particle in the downstream region, it will be trapped in this positive potential well. The presence of this potential peak is responsible for the dust particle attraction and alignment into the chains.

The results presented in this paper are in qualitative agreement with the potentials obtained with the help of PIC and LR methods [35]. However, in this paper, the potential peaks have much smaller amplitudes than the ones obtained

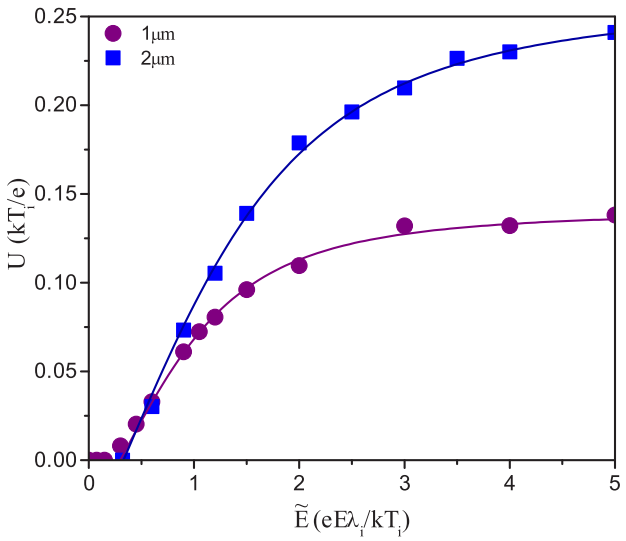

FIG. 9. Dependence of positive peak maximum $U_{\max}(z,\theta = 0)$ of $\widetilde{E}$ for different r_0.

in Ref. [35] because we considered dust particles with much smaller radii and charges.

IV. CONCLUSION

An alternative method of calculating plasma parameters around an isolated dust particle placed in an external electric field is developed. Ion trajectories are simulated by the Newtonian equations of ion motion taking into account the external electric field, the electric fields of the dust particle charge, and the volume charge of surrounding plasma. Ion-neutral collisions are simulated by the Monte Carlo method. A self-consistent electric potential is calculated iteratively with the help of Legendre polynomial expansions of the volume charge distribution. One peculiarity of the model is that the quasineutral condition is self-consistently fulfilled; i.e., the volume charge of the surrounding plasma totally screens the dust particle charge.

In the absence of the external electric field, the calculated dust particle charge and the ion density distribution around the dust particle show a good agreement with the previously developed models. The calculations of the plasma parameters around the dust particle are performed for different values of the external electric field and the particle radius. The model permits us to divide the ions into two groups, i.e., the trapped ions and the free ions. Without the external electric field, trapped ions play the main role in the screening and provide most of the volume charge. In the presence of the external electric field, trapped ions density decreases and the "quasiatom" is affected by the field ionization. For large electric fields, dust particles are screened mainly by free ions.

It was shown how the wake in the electric potential distribution begins to form downstream of the dust particle. This wake is mainly formed by the free ions. The value of the first maximum of the wake grows with the increase of the external field and has a saturation limit. The larger the dust particle radius, the higher its charge and the higher the saturation limit. The negatively charged particles will

be attracted by this potential well. Since this phenomenon is responsible for the dust particle alignment it must be thoroughly investigated for diverse plasma parameters.

ACKNOWLEDGMENT

This work was supported by the Russian Science Foundation (Grant No. 14-50-00124).

[1] P. K. Shukla, Phys. Plasmas **8**, 1791 (2001).
[2] R. L. Merlino and J. A. Goree, Phys. Today **57**(7), 32 (2004).
[3] V. E. Fortov, A. V. Ivlev, S. A. Khrapak, A. G. Khrapak, and G. E. Morfill, Phys. Rep. **421**, 1 (2005).
[4] O. Ishihara, J. Phys. D **40**, R121 (2007).
[5] J. H. Chu and Lin I, Phys. Rev. Lett. **72**, 4009 (1994).
[6] A. Melzer, T. Trottenberg, and A. Piel, Phys. Lett. A **191**, 301 (1994).
[7] H. Thomas, G. E. Morfill, V. Demmel, J. Goree, B. Feuerbacher, and D. Mohlmann, Phys. Rev. Lett. **73**, 652 (1994).
[8] H. Totsuji, T. Kishimoto, and C. Totsuji, Phys. Rev. Lett. **78**, 3113 (1997).
[9] U. Konopka, G. E. Morfill, and L. Ratke, Phys. Rev. Lett. **84**, 891 (2000).
[10] M. Bonitz, D. Block, O. Arp, V. Golubnychiy, H. Baumgartner, P. Ludwig, A. Piel, and A. Filinov, Phys. Rev. Lett. **96**, 075001 (2006).
[11] Z. Donko, G. J. Kalman, and P. Hartmann, J. Phys.: Condens. Matter **20**, 413101 (2008).
[12] C. Henning, H. Baumgartner, A. Piel, P. Ludwig, V. Golubnichiy, M. Bonitz, and D. Block, Phys. Rev. E **74**, 056403 (2006).
[13] C. Henning, K. Fujioka, P. Ludwig, A. Piel, A. Melzer, and M. Bonitz, Phys. Rev. Lett. **101**, 045002 (2008).
[14] T. Ott and M. Bonitz, Phys. Rev. Lett. **103**, 195001 (2009).
[15] H. Kahlert and M. Bonitz, Phys. Rev. Lett. **104**, 015001 (2010).
[16] P. Ludwig, H. Thomsen, K. Balzer, A. Filinov, and M. Bonitz, Plasma Phys. Control. Fusion **52**, 124013 (2010).
[17] M. Bonitz, Z. Donkó, T. Ott, H. Kählert, and P. Hartmann, Phys. Rev. Lett. **105**, 055002 (2010).
[18] F. Melandsø and J. Goree, Phys. Rev. E **52**, 5312 (1995).
[19] V. A. Schweigert, I. V. Schweigert, A. Melzer, A. Homann, and A. Piel, Phys. Rev. E **54**, 4155 (1996).
[20] K. Takahashi, T. Oishi, K.-i. Shimomai, Y. Hayashi, and S. Nishino, Phys. Rev. E **58**, 7805 (1998).
[21] D. S. Lemons, M. S. Murillo, W. Daughton, and D. Winske, Phys. Plasmas **7**, 2306 (2000).
[22] D. Winske, W. Daughton, D. S. Lemons, and M. S. Murillo, Phys. Plasmas **7**, 2320 (2000).
[23] S. A. Maiorov, S. V. Vladimirov, and N. F. Cramer, Phys. Rev. E **63**, 017401 (2000).
[24] I. V. Schweigert, V. A. Schweigert, and F. M. Peeters, Phys. Plasmas **12**, 113501 (2005).
[25] S. Khrapak and G. Morfill, Contrib. Plasma Phys. **49**, 148 (2009).
[26] I. H. Hutchinson, Plasma Phys. Control. Fusion **44**, 1953 (2002).
[27] I. H. Hutchinson, Plasma Phys. Control. Fusion **45**, 1477 (2003).
[28] I. H. Hutchinson, Plasma Phys. Control. Fusion **47**, 71 (2005).
[29] S. V. Vladimirov and M. Nambu, Phys. Rev. E **52**, R2172(R) (1995).
[30] A. Melzer, V. A. Schweigert, I. V. Schweigert, A. Homann, S. Peters, and A. Piel, Phys. Rev. E **54**, R46(R) (1996).
[31] M. Lampe, G. Joyce, G. Ganguli, and V. Gavrishchaka, Phys. Plasmas **7**, 3851 (2000).
[32] G. A. Hebner and M. E. Riley, Phys. Rev. E **69**, 026405 (2004).
[33] I. H. Hutchinson, Plasma Phys. Control. Fusion **48**, 185 (2006).
[34] I. H. Hutchinson, Phys. Plasmas **18**, 032111 (2011).
[35] P. Ludwig, W. J. Miloch, H. Kählert, and M. Bonitz, New J. Phys. **14**, 053016 (2012).
[36] G. I. Sukhinin, A. V. Fedoseev, and M. Salnikov, Contrib. Plasma Phys. **56**, 397 (2016).
[37] R. L. Dewar and D. Leykam, Plasma Phys. Control. Fusion **54**, 014002 (2012).
[38] R. Kompaneets, G. E. Morfill, and A. V. Ivlev, Phys. Rev. Lett. **116**, 125001 (2016).
[39] R. Kompaneets, G. E. Morfill, and A. V. Ivlev, Phys. Rev. E **93**, 063201 (2016).
[40] L. Patacchini and I. H. Hutchinson, Phys. Rev. Lett. **101**, 025001 (2008).
[41] I. H. Hutchinson, Phys. Rev. E **85**, 066409 (2012).
[42] I. H. Hutchinson and C. Haakonsen, Phys. Plasmas **20**, 083701 (2013).
[43] B. M. Smirnov, Phys. Scr. **61**, 595 (2000).
[44] S. A. Maiorov, Plasma Phys. Rep. **35**, 802 (2009).
[45] J. E. Allen, Phys. Scr. **45**, 497 (1992).
[46] A. V. Zobnin, A. D. Usachev, O. F. Petrov, and V. E. Fortov, Phys. Plasmas **15**, 043705 (2008).
[47] G. I. Sukhinin and A. V. Fedoseev, IEEE Trans. Plasma Sci. **38**, 2345 (2010).
[48] G. I. Sukhinin, A. V. Fedoseev, S. N. Antipov, O. F. Petrov, and V. E. Fortov, Phys. Rev. E **79**, 036404 (2009).
[49] M. Lampe, R. Goswami, Z. Sternovsky, S. Robertson, V. Gavrishchaka, G. Ganguli, and G. Joyce, Phys. Plasmas **10**, 1500 (2003).